

Vacuum arc deposition of Ti coatings

B. Straumal^{a,b,*}, W. Gust^a, N. Vershinin^{b,c}, R. Dimitriou^d, E. Rabkin^e

^a *Institut für Metallkunde, Seestrasse 92, D-70174 Stuttgart, Germany*

^b *I.V.T. Ltd, PO Box 47, 109180 Moscow, Russia*

^c *SONG Ltd., PO Box 98, Chernogolovka, Moscow District, 142432, Russia*

^d *Pechiney CRV, BP 27, 38340 Voreppe, France*

^e *Technion — Israel Institute of Technology, Department of Materials Engineering, Haifa 32000, Israel*

Abstract

Ti coatings on silicate glass substrates have been produced using a nonfiltered vacuum arc deposition technique. The dependence of the deposition rate and average roughness R_a on the discharge current and distance from the cathode was investigated. The deposition rate decreases monotonically with the distance and increases nonlinearly with the discharge current. R_a also increases with increasing discharge current. R_a decreases with the distance, showing a transition area between the microparticle-containing and microparticle-free Ti films. R_a depends strongly on the number of microparticles. A linear dependence of R_a on the distance was obtained only for substrates far enough from the cathode. For substrates close to the cathode the dependence is governed by the microparticle density. Therefore, the roughness can be changed in a very broad interval by changing the deposition parameters. © 2000 Elsevier Science S.A. All rights reserved.

Keywords: Deposition rate; Roughness; Titanium; Vacuum arc deposition

1. Introduction

Titanium is a transition metal mainly characterized by its high specific modulus and its good resistance to corrosion. Ti coatings are mainly attractive owing to their biocompatibility, which makes them reliable for the design of medical instruments or implants in the human body. The chemical and morphological modification of metallic implant materials has been shown by in vivo tests to influence their biocompatibility. The control of the surface roughness is an important factor for the implants [1,2]. Rougher surfaces have been shown to result in firmer bone fixation [3,4]. Vacuum arc deposition of titanium, though less documented than sputter deposition, offers a wide range of microstructural and morphological properties for coatings [5,6]. The cathodic arc plasma deposition process enables one to generate a much higher degree of ionization than other ion-plating processes, providing a better film adhesion and higher densities. Some 30 to 80% of the material that is evaporated from the cathode surface is ionized,

including multiply charged states [7,8]. The kinetic energies of the ions typically are in the 10 to 100 eV range. These features result in deposits of superior quality in comparison with other physical vapour deposition processes. High deposition rates can be achieved with an excellent coating uniformity. As a result of the arc process, microparticles are emitted at a very high velocity towards the substrate and contribute to the film formation. Though often considered as a disadvantage for applications in optics and electronics, the microparticles also represent a good way to create films of a given roughness [9]. The following study presents the main coating characteristics of vacuum arc deposited titanium on silicate glass as a function of deposition parameters. It gives a quantitative overview of the deposition rate and roughness values available for widely used titanium coatings.

2. Experimental

The vacuum arc apparatus used in this work is described elsewhere [10]. The facilities for magnetic filtering of the microparticles were not used in this work. Ti was deposited on a $450 \times 470 \times 4$ mm³ silicate glass

* Corresponding author. Tel.: +49-711-121-1276;
fax: +49-711-121-1280.

E-mail address: straumal@mf.mpi-stuttgart.mpg.de (B. Straumal)

plate. The glass plate was positioned horizontally, at the middle of the round cathode, perpendicular to the cathode surface plane, 50 mm away from it. The round cathode has a diameter of 180 mm. Before coating, a grid was drawn on the glass surface with the aid of an overhead pen. The grid provided a set of nodes located at a definite position relative to the cathode surface. The grid also acted as a mask and its removal after deposition made it possible to determine of the film thickness at each node. After deposition, the plate was cut into $40 \times 30 \text{ mm}^2$ samples suitable for the measurements. This experimental procedure ensures the similarity of the process conditions for each sample, the absence of sample shadowing and a large quantity of samples through one experiment. All data given in this work were obtained on the top surface of the substrate. The vacuum arc source voltage was maintained constant at $U=22 \text{ V}$ while the discharge current I varied ($I=110, 140, 160, 175$ and 220 A). No bias was applied to the substrate. The coating time t was the same for all samples ($t=420 \text{ s}$) except for $I=160 \text{ A}$ ($t=240 \text{ s}$). To prevent overheating of the surfaces, the 420 s coating process was divided into two coating periods (210 s each) separated by a 60 s interruption.

The sample surface was observed using a Zeiss Axiophot optical microscope and an Autoprobe CP AFM atomic force microscope (AFM) from Park Scientific Instruments. The thickness of the coatings d was measured with the aid of both a Taylor–Hobson Polystep profilometer and the AFM. During the thickness determination using profilometry six consecutive measurements of the step height between the coated and non-coated part were averaged. The average roughness R_a also was derived from profilometry measurements. The AFM was operated in the contact mode, using sharpened gold-coated microlevers with a nominal radius of the tip curvature of less than 20 nm. For the film thickness measurements $50 \times 50 \mu\text{m}^2$ scans were positioned in such a way that the border between coated and uncoated glass was approximately in the middle of the scanned area. The thickness was then determined as an average from four line scans that were not disturbed by the particles or contaminations at the coated/uncoated glass border. The profilometer thickness measurements were known within a 5% accuracy, and the AFM enabled one to measure the thickness with an accuracy of 5 nm.

3. Results and discussion

Figs. 1–3 display the microstructure of the Ti coatings. During vacuum arc deposition, the flux of material coming from the cathode to the substrate contains multiply charged ions and microdroplets [11]. The microdroplets are thought to be ejected from the liquid

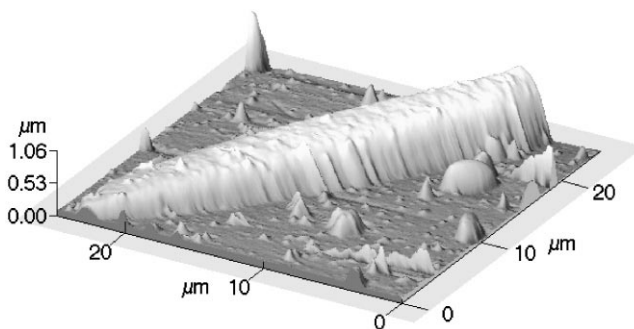


Fig. 1. AFM low magnification micrograph of vacuum arc deposited Ti coating on the silicate glass substrate ($L=80 \text{ mm}$, $I=160 \text{ A}$, $t=240 \text{ s}$) showing the 'tail' of a big droplet, smaller droplets and smooth film formed from ionic flux.

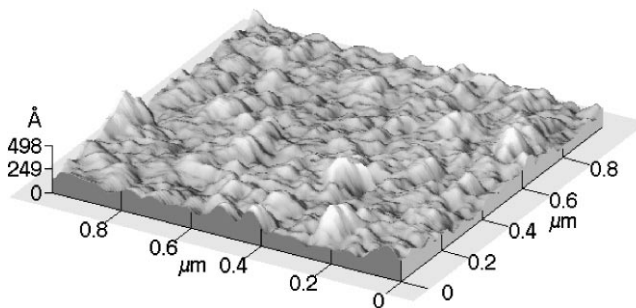


Fig. 2. AFM high magnification micrograph of vacuum arc deposited Ti coating on the silicate glass substrate ($L=80 \text{ mm}$, $I=160 \text{ A}$, $t=240 \text{ s}$) showing the topography of a film between droplets.

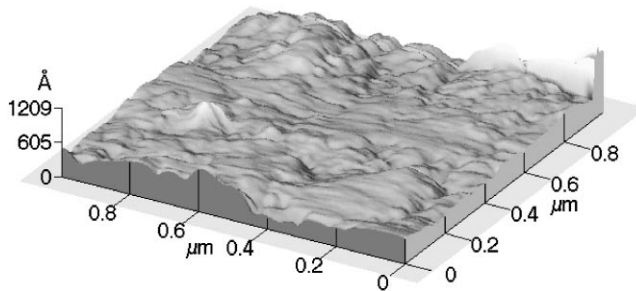


Fig. 3. AFM high magnification micrograph of vacuum arc deposited Ti coating on the silicate glass substrate ($L=80 \text{ mm}$, $I=160 \text{ A}$, $t=240 \text{ s}$) showing the surface topography of a droplet.

pool of the cathode (created by the arc impact) by the ionic flux accelerated back towards the target [12]. The microdroplets are usually emitted at low angles relative to the cathode surface [13], but some are also found normal to the cathode surface [14]. Their shape depends mostly on the angle between their trajectory and the substrate plane. In our case, the microdroplets fly almost parallel to the substrate plane. Their resulting shape is thus ellipsoidal and can be characterized by their aspect ratio. The surface morphology is driven mainly by the microparticle density. Close to the cathode, the Ti film has a very rough surface made of overlapping microparticles. In this zone, the dark grey coating has a poor

adherence to the glass substrate. The droplets have various sizes and shapes, from nearly circular to elongated. Further away from the cathode, both droplets and a homogeneous film formed by deposition of individual ions can be clearly seen. The microdroplets are still of various sizes but their shape is more uniform. The average aspect ratio is higher and leads to a standard elongated shape. In the AFM picture made with a low magnification the ‘tail’ of a large microdroplet is visible together with some smaller particles on the rather smooth surface of a film formed by the flux of individual ions. The homogeneity in droplets shape and direction reveals a better uniformity of the particle flux compared with the near-cathode zone. High-magnification AFM pictures show the smooth film between the droplets (Fig. 2) and the surface morphology of the microdroplets (Fig. 3). The average roughness R_a measured profilometrically on the length of 80 μm includes both big and small droplets and a smooth surface among them and, therefore, is rather high (about 350 nm on the sample shown in Figs. 1–3). R_a measured microscopically is much lower (3.6 nm for the location shown in Fig. 2 and 5.5 nm for Fig. 3). If the deposition process is carried on, the microdroplets become a part of the coating. Their structure may or may not differ from the film itself [9,15]. At the largest distance from the cathode, the microdroplets occurrence is very low and the coating consists of a homogeneous film formed by deposition of individual ions and which can be considered as microparticle free. The AFM measurements reveal that the film among the particles is atomically smooth ($R_a = 1 \text{ nm}$) at $L > 200 \text{ mm}$.

The dependence of deposition rate R_d on the transverse distance d_t is shown in Fig. 4 for different distances $L = 170$ and 230 mm from the cathode. Both curves are symmetric, having the maximum at the middle of the substrate where $d_t = 0$. R_d decreases monotonically with increasing d_t . The dependence of deposition rate

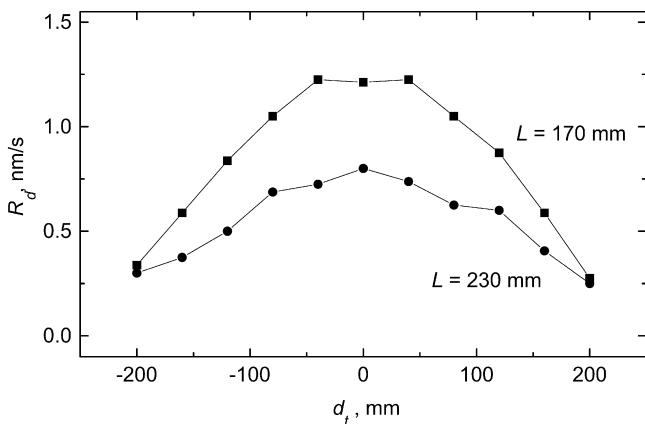


Fig. 4. Dependence of the Ti deposition rate R_d on the transverse distance d_t from the symmetry axis of the substrate for different distances L to the cathode. Deposition time $t = 240 \text{ s}$.

R_d on discharge current I is shown in Fig. 5 for various distances L from the cathode. The R_d values were measured along the middle line of the substrate ($d_t = 0$), being, therefore, the maximal values for each L . The $R_d(I)$ curves show linearity only for samples far enough from the cathode. Close to it, the microparticles presence boosts the deposition rate and a sharp variation with the discharge current I is observed. As can be seen from Fig. 5, R_d decreases monotonically with increasing L at a fixed discharge current I . The decrease is rather slow, especially at high I . The low variation of R_d with increasing distance illustrates the high throwing power of the arc process [5]. It has been already noticed [16] that for cathodic arc evaporation R_d decreases slower with increasing L than in the case of magnetron sputtering. This allows one to coat effectively three-dimensional parts having a complicated form. The slow $R_d(L)$ dependence is also advantageous for the coating of planar large-area substrates, allowing one to transport the frames with substrates at various distances from the cathode. This feature allowed one to simplify the construction of the vacuum arc deposition apparatus for large-area substrates [17]. The deposition rates for Ti close to the cathode surface are quite high, with values up to 9 nm/s for $I = 220 \text{ A}$ and $L = 80 \text{ mm}$. For Ti films deposited on stainless steel plates placed 160 mm from the cathode, Martin et al. [6] found $R_d = 5 \text{ nm/s}$ at $I = 90 \text{ A}$. In our case an estimated value $R_d = 2 \text{ nm/s}$ is found. The difference may be explained by the fact that the substrates in Ref. [6] are oriented parallel to the cathode surface, whereas here the substrates lie perpendicular to it, and R_d values for substrates parallel to the cathode surface are usually much higher than for those oriented perpendicular to the cathode plane [10,16].

The dependence of R_a (measured by profilometry at a length of 80 μm) on the distance L from the cathode for various values of the discharge current I is shown in

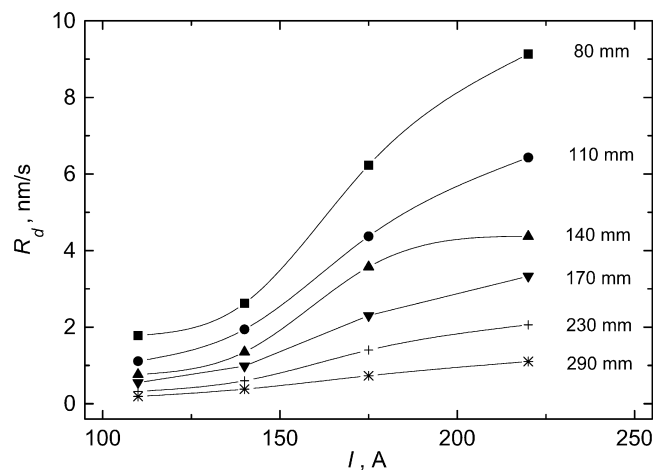


Fig. 5. Dependence of the Ti deposition rate R_d on the discharge current I for different distances L to the cathode along the symmetry axis of the substrate ($d_t = 0$). Deposition time $t = 420 \text{ s}$.

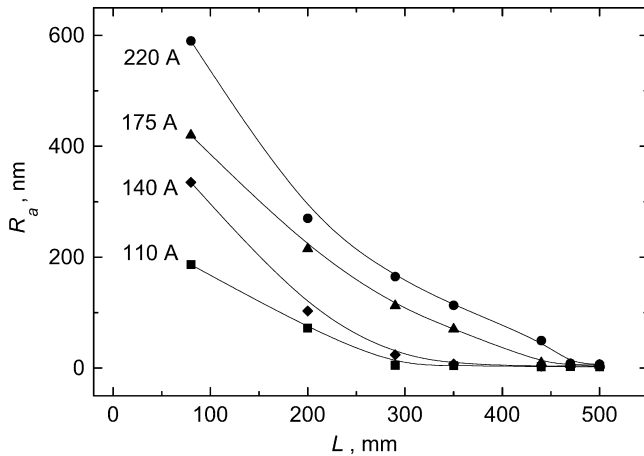


Fig. 6. Dependence of the average roughness R_a on distance L to the cathode for different values of discharge current I measured along the symmetry axis of the substrate ($d_t=0$). Deposition time $t=420$ s.

Fig. 6. These data were also measured along the middle line of the substrate ($d_t=0$). For samples close to the source, R_a sharply decreases with the distance L . The surface is built of micrometre-sized overlapping particles. Values up to 600 nm are found. Further away, as the film begins to be free from microparticles, R_a goes down to about 4 nm, which is the initial roughness of the glass substrate. The numerical significance of R_a for these samples is the average of a rather smooth background on which the microparticles are randomly dispersed. A more detailed description of the surface morphology would imply a bimodal roughness description [18]. An increase of the discharge current I increases the roughness and widens the choice of available roughnesses. The higher the discharge current, the larger the microparticle-free zone. For comparison, in the biomedical field, reported R_a values needed for bone anchoring on implants range from 460 to 8400 nm [19,20]. The deposition time t is the third parameter that enables one to produce a given roughness, but its influence has not been studied here. Comparison of the data given in Figs. 5 and 6 shows that there is no linear correlation between R_d and R_a . Namely, the deposition rate decreases much more slowly with increasing L and decreasing I than the average roughness. This is very important from the technological point of view, because it allows one to obtain very smooth coatings on a substrate with a reasonable deposition rate simply by increasing the distance from the cathode.

Acknowledgements

The financial support of the NATO Linkage Grant (contract HTECH.LG.970342+ CN.SUPPL 973216), the Isopress-Inter Programme of the Russian Ministry of Science and Technology, Royal Swedish Academy of Sciences and the Copernicus Networks (contracts ERB IC15 CT98 0815 and ERB IC15 CT98 0812) is acknowledged.

References

- [1] T. Albrechtsson, P.-I. Brenemark, H.-A. Hansson, J. Lindström, *Acta Orthop. Scand.* 52 (1981) 155.
- [2] T. Peltola, M. Patsi, R. Viitala, I. Kangasniemi, A. Yli-Urpo, S. Kothari, P. Hatton, in: L.A.J.L. Sarton, H.B. Zeedijk (Eds.), *Materials Functionality and Design* vol. 3, The Netherlands Society for Materials Science, Zwijndrecht, 1997, p. 569.
- [3] D. Buser, R.K. Schenk, S. Steinemann, J.P. Fiorellini, C.H. Fox, H. Stich, *J. Biomed. Mater. Res.* 25 (1991) 889.
- [4] L. Carlsson, T. Rustlund, B. Albrechtsson, T. Albrechtsson, *Int. J. Oral Maxillofac. Implants* 3 (1988) 21.
- [5] P.J. Martin, D.R. McKenzie, R.P. Netterfield, P. Swift, S.W. Filipczuk, K.H. Müller, G. Pacey, B. James, *Thin Solid Films* 153 (1987) 91.
- [6] P.J. Martin, P. Netterfield, D.R. McKenzie, I.S. Falconer, C.G. Pacey, P. Tomas, G. Sainty, *J. Vac. Sci. Technol. A* 5 (1987) 22.
- [7] I.G. Brown, J.E. Galvin, *IEEE Trans. Plasma Sci.* 17 (1989) 679.
- [8] I.G. Brown, X. Godechot, *IEEE Trans. Plasma Sci.* 19 (1991) 713.
- [9] B. Straumal, N. Vershinin, V. Semenov, V. Sursaeva, W. Gust, *Defect Diff. Forum* 143–147 (1997) 1637.
- [10] N. Vershinin, B. Straumal, W. Gust, *J. Vac. Sci. Technol. A* 14 (1996) 3252.
- [11] R.L. Boxman, P.J. Martin, D.M. Sanders (Eds.), *Handbook of Vacuum Arc Science and Technology*, Noyes Publications, Park Ridge, NJ, 1995, p. 367.
- [12] G.W. McClure, *J. Appl. Phys.* 45 (1974) 2078.
- [13] J.E. Daadler, *J. Phys. D* 8 (1975) 1647.
- [14] J.E. Daadler, *J. Phys. D* 9 (1976) 2379.
- [15] B.B. Straumal, N.F. Vershinin, R. Dimitriou, W. Gust, T. Watanabe, Y. Igarashi, X. Zhao, *Thin Solid Films* 319 (1998) 127.
- [16] N.F. Vershinin, V.G. Glebovsky, B.B. Straumal, W. Gust, H. Brongersma, *Appl. Surf. Sci.* 109–110 (1997) 437.
- [17] B. Straumal, N. Vershinin, K. Filonov, R. Dimitriou, W. Gust, *Thin Solid Films* 351 (1999) 190.
- [18] H.G. Pfaff, G. Willmann, *Interceramics* 43 (1994) 73.
- [19] T.J. Vijayaraghavan, A. Bensalem, *J. Mater. Sci. Lett.* 13 (1994) 1782.
- [20] K. Hayashi, T. Inadome, H. Tsumura, Y. Nakashima, Y. Sugiooka, *Biomaterials* 15 (1994) 1187.